Preparation of colloidal silver dispersions by the polyol process

Part 2.† — Mechanism of particle formation

Pierre-Yves Silvert,*[a] Ronaldo Herrera-Urbina[b] and Kamar Tekaia-Elhsissen[a]

[a]*Laboratoire de Réactivité et de Chimie des Solides, URA CNRS 1211, Université de Picardie Jules Verne, 33, rue Saint-Leu, 80039 Amiens Cedex, France*

[b]*Universidad de Sonora, Departamento de Ingenieria Quimica y Metalurgia, 83000 Hermosillo, Sonora, Mexico*

In a previous paper (*J. Mater. Chem.*, 1996, **6**, 573), we reported that colloidal silver dispersions can be synthezised by the polyol process, using an ethylene glycol–polyvinylpyrolidone (PVP) solution to reduce silver nitrate under precise temperature conditions. Quasi-spherical particles with a narrow size distribution were obtained. Low precursor and PVP concentrations, in contrast to high silver nitrate concentrations, were found to yield monodisperse systems with an average particle size of 15 to 21 nm. To understand the particle formation mechanism, the evolution of particle size and shape during the reaction was monitored by TEM and UV absorption spectroscopy techniques. An Ostwald ripening mechanism is proposed to account for the formation of the silver particles, even though the variation of temperature with time is not ideal for a complete mechanistic understanding.

New methods for the synthesis of noble metal dispersions are frequently reported in the literature. Metal colloids can be produced in both aqueous and non-aqueous solvents. In this field, the preparation of silver colloids is very well known and well developed: several preparations have been made in organic solvents.[1] Silver colloids have been formed in acetonitrile[2] and propan-2-ol[3] by reducing a silver compound in the presence of a protective agent.

As a matter of fact, this increasing interest in small metal particles is related to the unique properties exhibited by these systems which result from size effects: particle size dependence on electronic susceptibility and magnetic resonance relaxation,[4,5] high surface area and exceptional surface activity. Nanomaterials therefore have many applications in physics, chemistry, biology and medicine; they are ideal catalysts for many organic reactions and potential candidates for use as advanced materials. However, colloidal dispersions must meet very strict requirements of particle size, uniform shape and narrow size distribution.

As reported previously, we have prepared colloidal silver dispersions with a narrow size distribution, by adaptation of the polyol process,[6] using ethylene glycol solutions of silver nitrate and polyvinylpyrrolidone (PVP). The obtained colloids and their characteristics are presented in Table 1.

In order to understand the mechanism of particle formation, we decided to monitor the evolution of particle size and shape during the reaction and to study the influence of reaction parameters such as temperature, time and PVP concentration, in the case of one particular precursor mass of 400 mg.

Experimental

Materials

The precursor used to synthesize colloidal silver was silver nitrate (Rectapur). Reagent-grade ethylene glycol was used as the solvent for $AgNO_3$ and as the reducing agent. Polyvinylpyrrolidone (PVP K15, M_r 10000) was used as the protecting agent. These reagents were purchased from Prolabo and were used without further purification.

Preparation of the colloids and reaction monitoring

Experiments were carried out under the same conditions as in Part 1 of this study:[6] PVP (4, 7, 10 or 12 g) was dissolved in 75 cm^3 ethylene glycol at room temperature, and 400 mg $AgNO_3$ (2.4 mmol) was added to this solution. The suspension was then stirred at room temperature until complete dissolution of the silver nitrate. Then, the system was heated to 120 °C at a constant rate of 1 °C min^{-1}, and the reaction allowed to proceed for 22 h at this temperature. Samples (*ca.* 1 cm^3 each) were taken during solution heating and until the end of the reaction, as shown in Table 2.

Each sample was cooled rapidly in a water bath until the system reached room temperature, and diluted with H_2O in a gauged flask up to 250 cm^3. The resulting solutions were used for the characterization studies.

Table 1 Colloidal silver dispersions obtained by the polyol process

$AgNO_3$/mg; mmol	PVP/g	mean size/nm	S.D.[a] (%)
50; 0.3	1.5	15	18
200; 1.2	7	20	17
400; 2.4	10	21	16
1000; 6.0	15	25	22
3200; 19.2	20	36	30

Table 2 Relationship between sample number, time and temperature during the reaction

sample number	t/h	T/°C
1	0.25	39
2	0.50	53
3	0.75	70
4	1.00	84
5	1.25	99
6	1.60	120
7	1.83	120
8	2.10	120
9	2.33	120
10	2.60	120
11	4.60	120
12	7.60	120
13	23.6	120

† Part 1, ref. 6.

Characterization

Every sample was characterized by transmission electron microscopy using a STEM CM12 Philips microscope. Samples for observation under the microscope were prepared by placing a drop of the colloidal silver dispersion onto a standard microscope grid coated with a carbon film. The mean particle size of colloidal silver and the standard deviation of particle population were determined from image analyses of the micrographs of these particles. Each colloidal sample was characterized by UV spectroscopy with a UVIKON 930 UV spectrophotometer from Kontron Instruments, with a variable radiation wavenumber between 300 and 800 nm. The presence of Ag^0 in solution is related to a broad absorbance peak whose maximum occurs at 410 nm.[3] The height of this peak gives direct information about the metallic silver concentration in the medium. As a matter of fact, our colloidal dispersions follow the Lambert–Beer law ($A = \varepsilon lc$). The 410 nm peak height is then directly proportional to the quantity of Ag^0 present in solution. By following its evolution during the reaction, we can estimate the rate of reduction of silver nitrate. The peak height at the end of the reaction is considered as a reference for 100% silver reduction; it is then possible to estimate the silver reduction rate (%) for any sample during colloidal silver formation. A peak corresponding to the Ag^+ species should be observed in the 200–300 nm region, but the peak due to the presence of organic species in solution overlaps with the Ag^+ peak, which cannot therefore be detected and quantified. The X-ray diffraction patterns were obtained with a Siemens D5000 diffractometer using Cu-$K\alpha_1$ radiation with an incident-beam-curved crystal germanium monochromator and asymmetric focusing. High-resolution electron microscopy observations were performed with a JEOL 200 CX microscope.

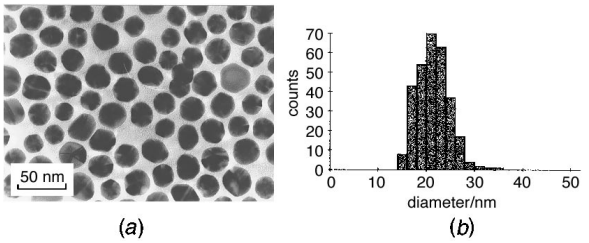

Fig. 1 (*a*) Transmission electron micrograph of a monodisperse silver dispersion. (*b*) Mean particle size 21.4 ± 3.3 nm, standard deviation 16%

Results

We chose to start working on the reaction mechanism with one of our monodisperse colloids, namely the silver dispersion with 21 nm particles and a standard devaition of *ca.* 16% (Fig. 1). The reaction was followed and the samples characterized as explained in the previous section. The stack histograms corresponding to all the samples are presented in Fig. 2, and the UV spectra are presented in Fig. 3.

In order to have a general view of the system evolution, the results obtained for all samples are summarized in Fig. 4. The variation of the mean particle size as a function of time has been plotted together with the variation of the absorbance peak at 410 nm, which is proportional to the metallic silver concentration in solution.

Fig. 4 consists of three different regions corresponding to the three main steps of the reaction. These steps are illustrated by the micrographs in Fig. 5.

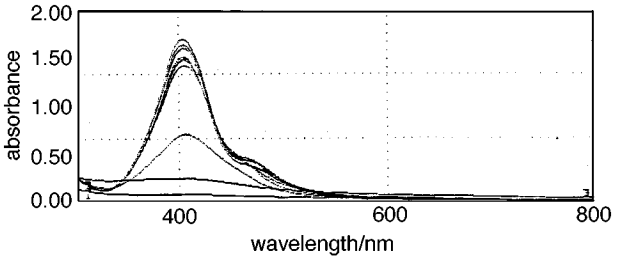

Fig 3 Evolution of UV spectra (410 nm peak) during the formation of monodisperse silver colloids with an average particle size of 21 nm (10 g PVP)

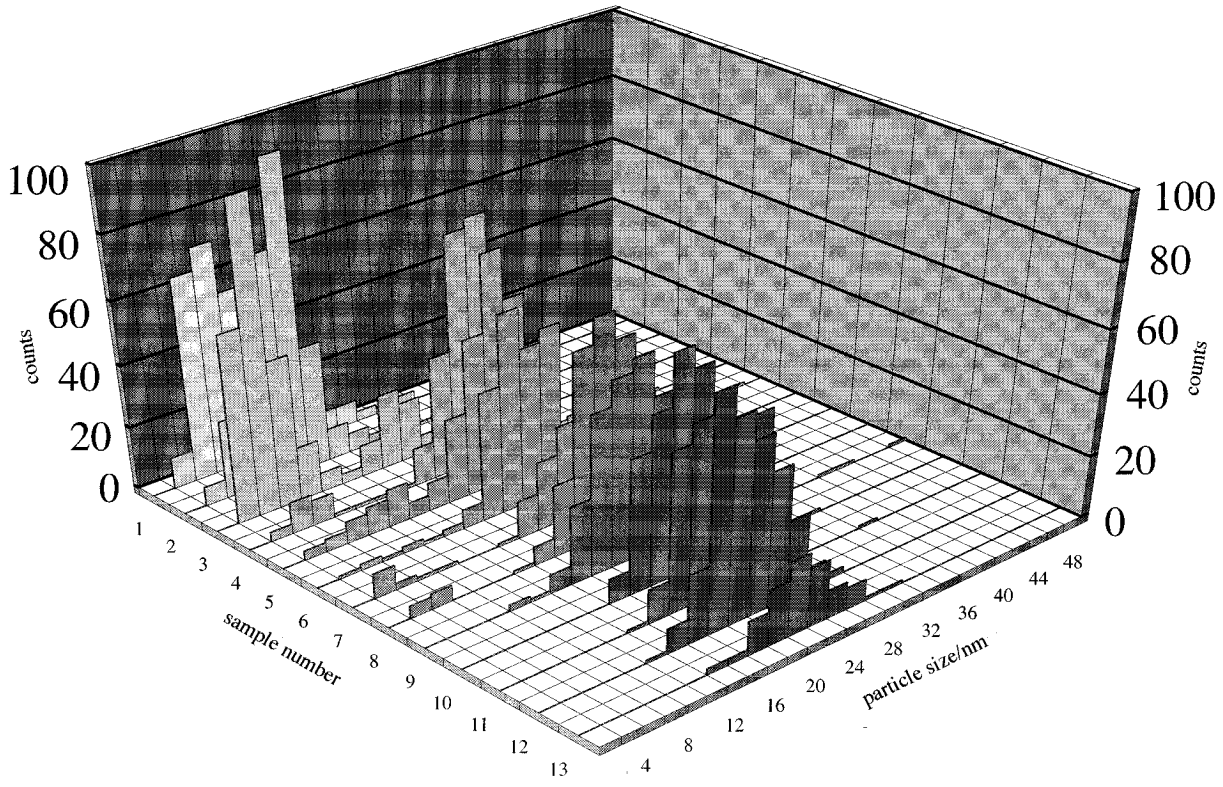

Fig. 2 Evolution of particle size distribution during the formation of monodisperse silver colloids with an average particle size of 21 nm (10 g PVP)

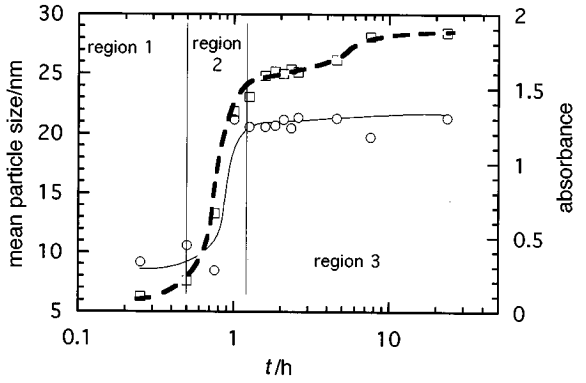

Fig. 4 Evolution of mean particle size (○) and absorbance peak (□) (at 410 nm) during the formation of 21 nm monodisperse silver colloids (10 g PVP)

Step 1. Silver nitrate slowly begins to react (8% of the total metallic silver present at the end of the reaction has appeared since the reaction beginning): the system is unstable and the quasi-spherical particles exhibit a heterogeneous distribution; after 15 min reaction ($T=39\,^{\circ}C$), the particles are small, with a mean size of less than 10 nm. However, it is noticeable that some large particles (5% of total population, mean size 21 nm corresponding to the final mean size of the colloid) have formed during the first step of the reaction. The standard deviation is high (*ca.* 40–50%).

Step 2. After 45 min of reaction ($T=70\,^{\circ}C$), a double particle size population appears: the majority are small particles (mean size 5 nm) and *ca.* 24% of large particles (mean size 18 nm) are present, with a very high standard deviation (70%). At $t=$ 60 min ($T=84\,^{\circ}C$), a very fast evolution of the system takes place: a spectacular shift results in the large particles forming the majority, with a noticeable decrease of the standard deviation (26%). The small particles quickly disappear to the benefit of the large ones. The system (*ca.* 8% particles with a mean size of 6 nm, and the majority of particles with a mean size of 21 nm) begins to stabilize despite the presence of residual small particles. The final mean size of the colloidal particles is reached at the end of this phase. Simultaneously, reduction shows an important acceleration: at the end of this step, 87% of the final metallic silver has been reduced, which corresponds to the shift in the particle population and the formation of a majority of large particles.

Step 3. From the previous point until $t=155$ min (after 1 h at 120 °C, sample no. 10), the system continues to evolve: the residual small particles disappear progressively, while the mean size remains stable. The standard deviation decreases until no more small particles are observed and the monodisperse colloid

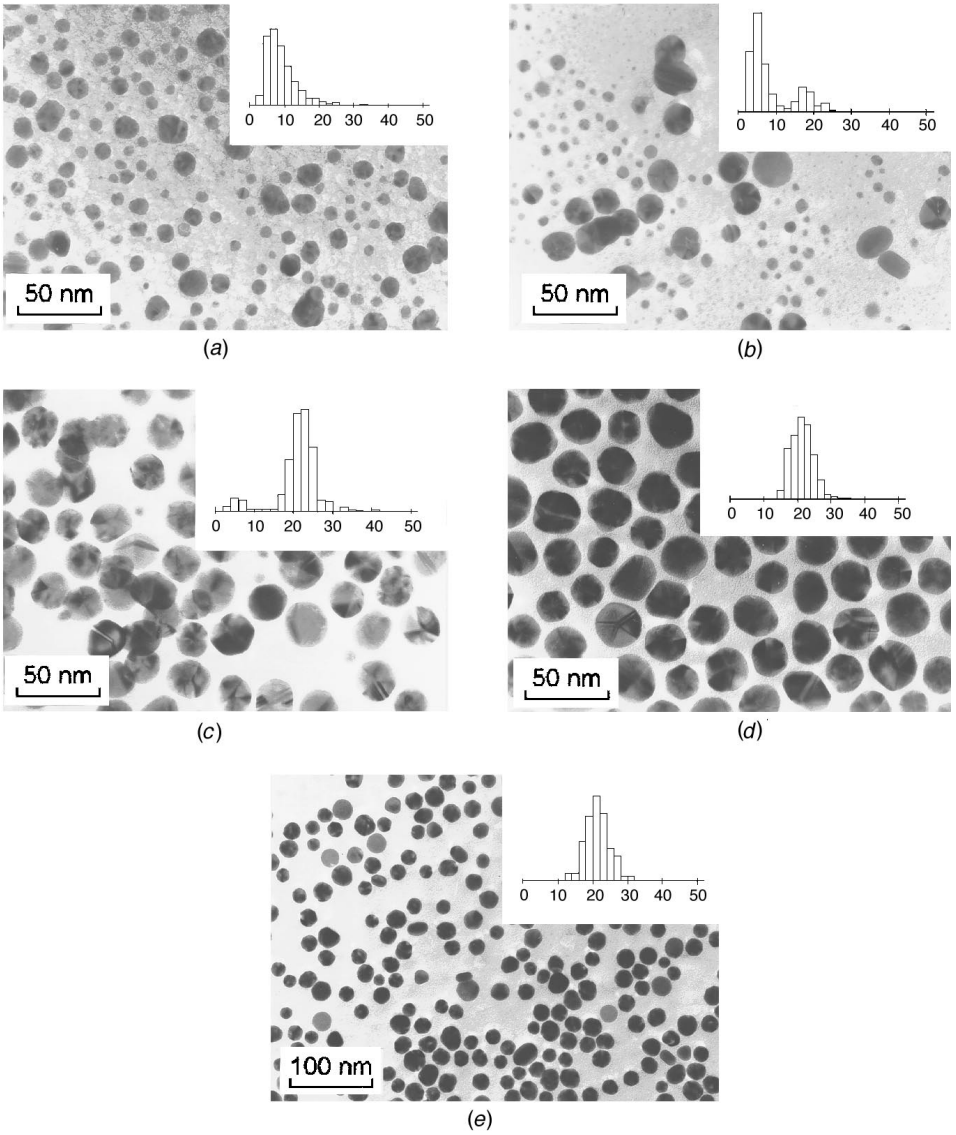

Fig. 5 Transmission electron micrographs of a colloidal silver dispersion at different stages of the reaction: (*a*) sample 1, (*b*) sample 3, (*c*) sample 4, (*d*) sample 10, (*e*) sample 13

is stable with a mean size of 21 nm and a variation coefficient of 16%. It is important to note that after 95 min of reaction, the absorbance curve reaches a plateau.

As the solution is kept at 120 °C, the mean particle size and the standard deviation remain stable. The system remains monodisperse until the end of the reaction (22 h at 120 °C). The micrograph does not permit the determination of a significant change in the mean particle size.

Influence of PVP concentration

PVP plays an important role in the protection of the synthesized particles, but it has also been found to act as a reducing agent.[16] It has been reported to reduce ammoniacal silver[7] and to promote nucleation. As a matter of fact, PVP is a homopolymer whose individual unit contains an imide group. The N and O atoms of this polar group probably have a strong affinity for silver ions and metallic silver.[8] A PVP macromolecule in solution, which most probably adopts a pseudo-random coil conformation, may take part in some form of association with the metal atoms, thus increasing the probability of nucleus formation. The role of amphiphatic dispersants in dispersion polymerization has been explained in similar terms.[9]

In order to gain a better insight into our reactions, we decided to study the influence of PVP concentration on particle formation, under the same conditions as previously, with different PVP additions: 4, 7 and 12 g. These experiments were sampled in the same way as described before (Table 2) and are compared with the previous results in the following paragraphs.

The stack histograms showing the evolution of particle size distribution are presented in Fig. 6 (4 g PVP), Fig. 7 (7 g PVP) and Fig. 8 (12 g PVP).

As in the case of the first experiment with 10 g PVP, the UV spectra of all samples are presented together in Fig. 9 for experiments with 4, 7 and 12 g PVP.

The effect of PVP concentration on mean particle size and absorbance is presented in Fig. 10 and 11.

The protective role of PVP is noticeable (Fig. 10), since at low PVP concentrations (4 and 7 g PVP) the colloids obtained are not monodisperse and the evolution of mean particle size is not regular. Small particles are always present in the system and the concentration of PVP is not high enough to regulate particle size distribution. During the reaction, some large particles are not protected by PVP and go on growing as silver nitrate reduces (Fig. 6 and 7). A higher PVP concentration (12 g PVP) permits the production of another monodisperse colloid whose particles seem to behave in exactly the same way as they do when a 10 g PVP addition is used. The 12 g PVP colloid gives approximately the same particle size with a narrow particle size distribution.

PVP indeed plays a reducing role: in Fig. 11, we can see a faster increase of the characteristic silver peak in the early stages of the reaction with increasing PVP concentration: silver nitrate reduces faster when more PVP is present.

Discussion

All four experiments conducted for this work show similar behaviour: at the beginning of the reaction, the majority of particles present are small, with a few large ones. At the end of the reaction, the systems consist mainly of large particles, whether the colloid is monodisperse or not. How do the large particles form during the reaction? The relation between the control of nucleation and growth and the monodispersity of the final powder has been described and explained by La Mer and Dinegar:[10] the production of monodisperse colloids results when the nucleation step is fast enough and the growth step does not interfere with the nucleation step. PVP plays a major role in the silver nitrate reduction: high concentrations lead to monodisperse colloids as PVP seems to enhance and shorten the nucleation step, as can be seen observable in experiments with 10 and 12 g PVP. In the case of experiments with 4 and 7 g PVP, nucleation and growth take place at the same time, producing polydisperse systems. Fig. 11 shows clearly that at the end of step 2, the reduction rate is PVP dependent: a low PVP concentration does not permit the formation of a short

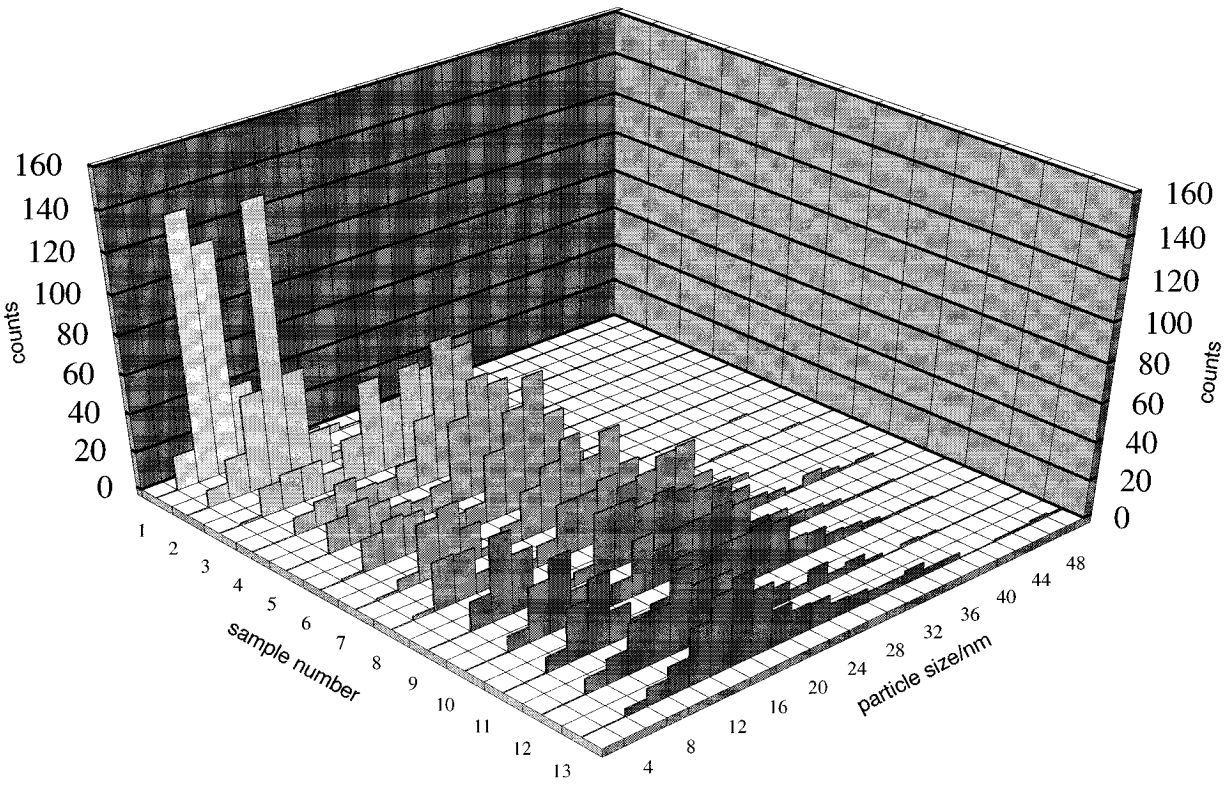

Fig. 6 Evolution of particle size distribution as a function of time (4 g PVP)

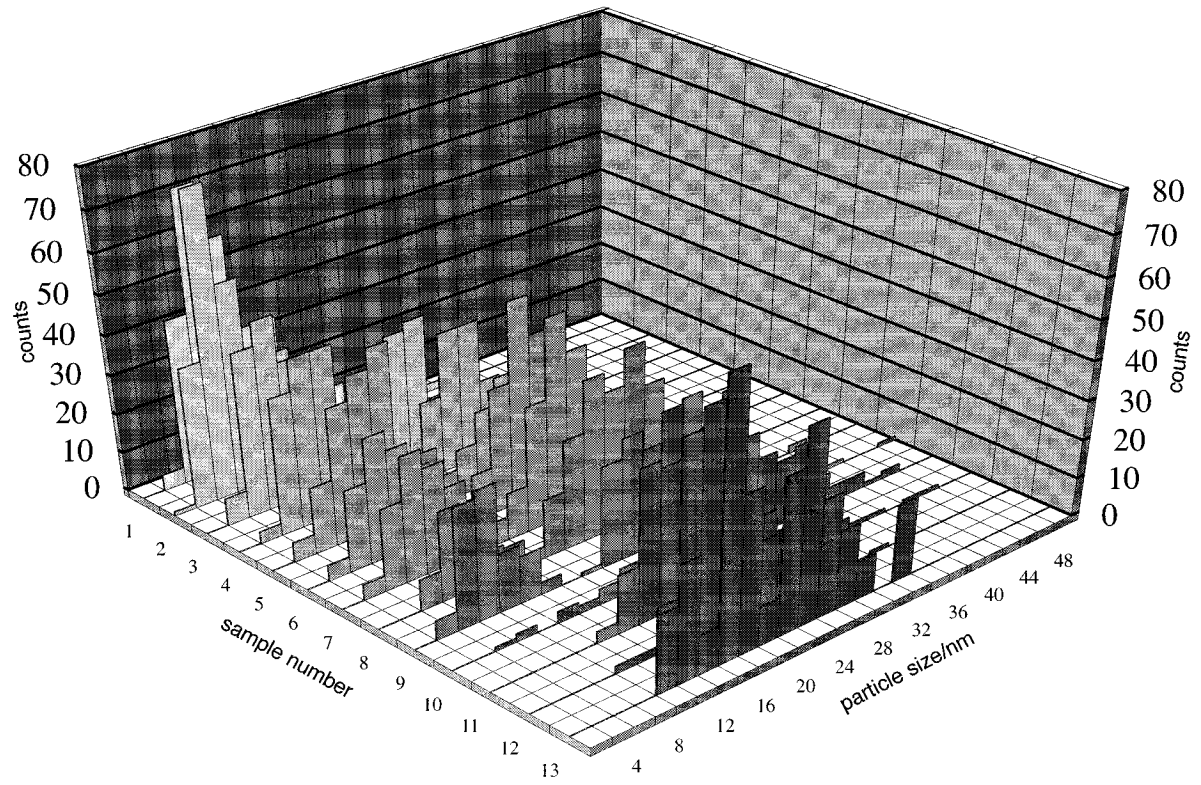

Fig. 7 Evolution of particle size distribution as a function of time (7 g PVP)

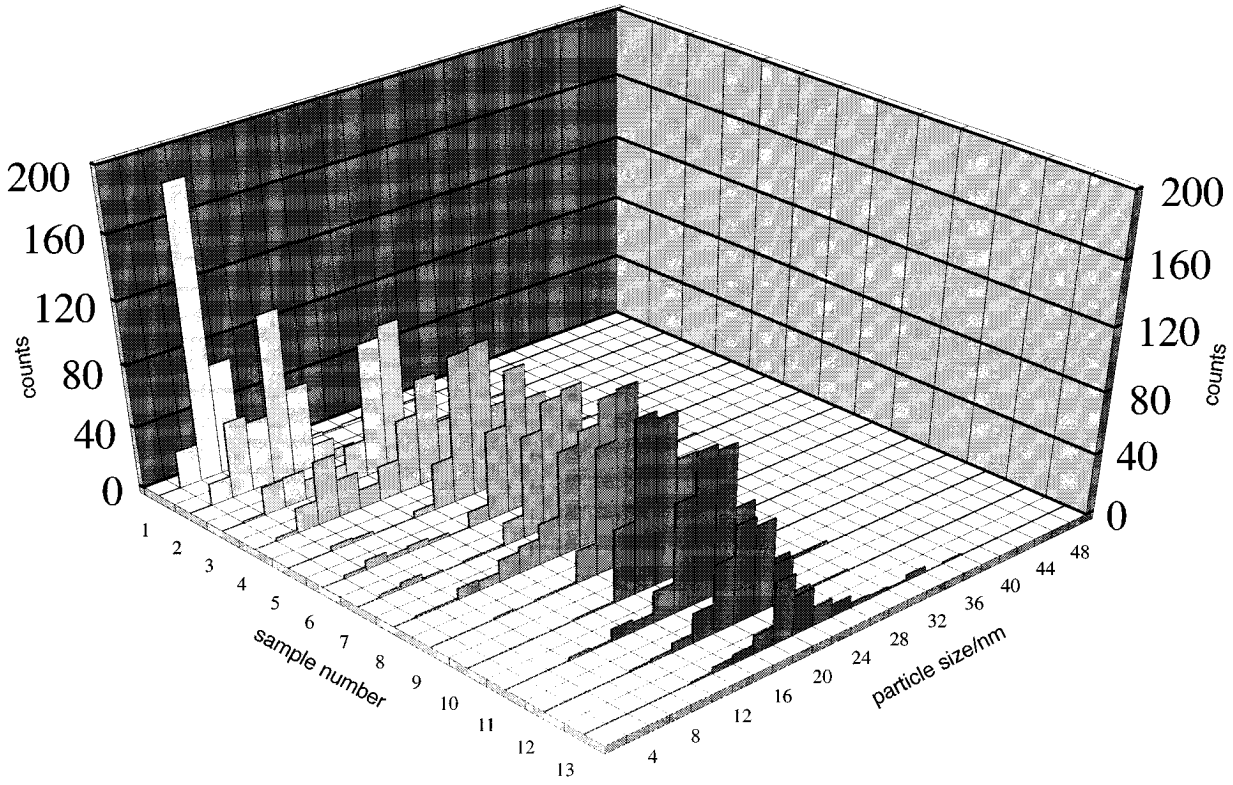

Fig. 8 Evolution of particle size distribution as a function of time (12 g PVP)

enough nucleation period, so nucleation continues during the growth step.

It is remarkable that the reaction steps described in Fig. 4 take place at the same time for all experiments (Fig. 11): PVP accelerates the reduction of silver ions during step 2.

Precious metals are known for their ability to sinter at relatively low temperatures when synthesized in organic or inorganic media.[11] It is possible, therefore, that the original small particles sinter during the reaction in order to form larger ones.

As we work at relatively high temperatures (120 °C), the formation of the larger particles could be the result of particle–particle sintering during the reaction. Close observation of the transmission electron micrographs does not reveal any sintered particles (Fig. 5). As a first attempt to throw some light on this issue, X-ray diffraction patterns of our colloidal silver

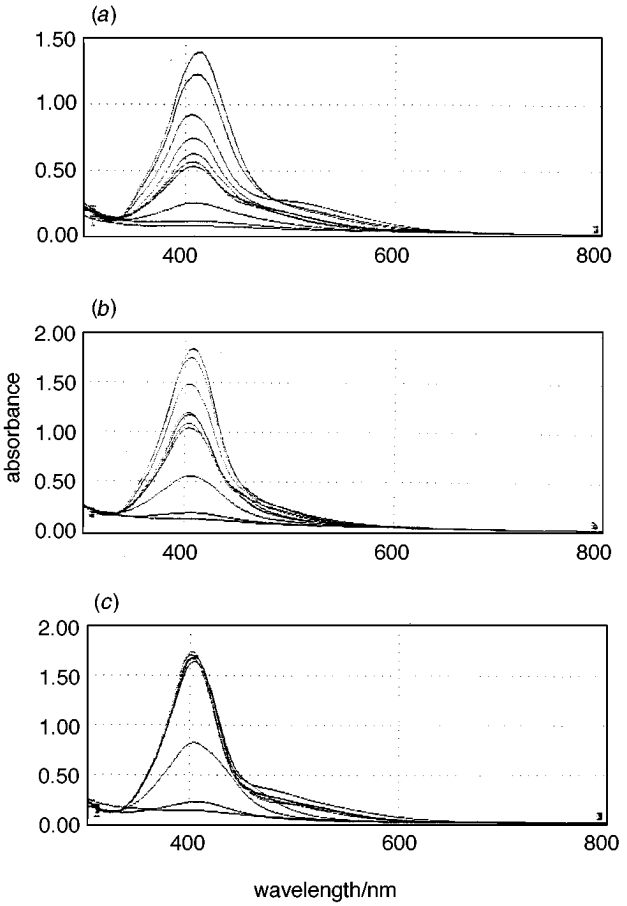

Fig. 9 UV spectra of colloidal dispersions during silver formation: (*a*) 4 g PVP, (*b*) 7 g PVP, (*c*) 12 g PVP

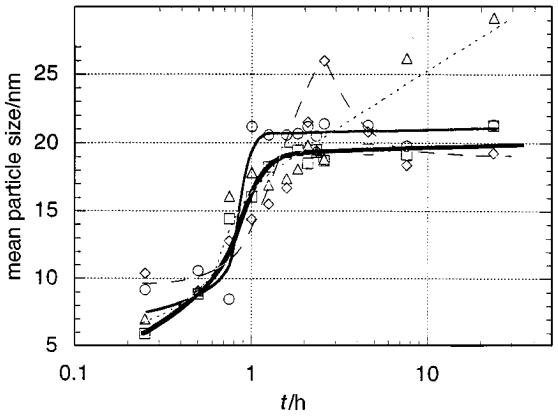

Fig. 10 Evolution of mean particle size during the formation of silver colloids: influence of PVP concentration (△, 4 g; ◇, 7 g; ○, 10 g; □, 12 g PVP)

dispersions were taken. Fig. 12 shows a typical example of such diffraction patterns. The powder exhibits good crystallinity. The mathematical deconvolution of the peaks permitted the calculation of the crystallite sizes using the Scherrer formula.[12] The result for the [1 1 1]* direction is a crystallite size of 11 nm. This approximate value is comparable to the mean particle sizes calculated by image analyses of our colloids (*ca.* 20 nm). As the Scherrer formula always tends to underestimate the real crystallite size,[12] this result seems to favour the hypothesis of the monocrystallinity of the particles. However, in order to ensure this, we observed our particles using high resolution electron microscopy. Fig. 13 shows an example of a silver particle: the shape is polyhedral and it is possible to

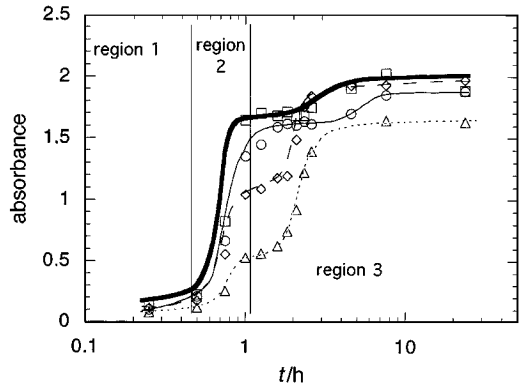

Fig. 11 Evolution of absorbance peak during the formation of silver colloids: influence of PVP concentration (△, 4 g; ◇, 7 g; ○, 10 g; □, 12 g PVP)

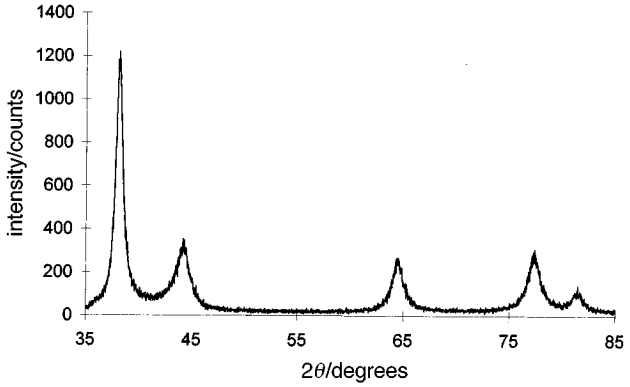

Fig. 12 Typical X-ray diffraction pattern of a collidal silver dispersion

observe that the particle is multiply twinned and can be represented schematically as a decahedron. Other observed particles exhibit an icosahedral shape. These observations are in agreement with those reported in the literature[13–15] and prove that our particles are monocrystalline and polyhedral. In our reactions, the particles formed are protected by PVP which acts as a steric stabilizer, inhibiting their agglomeration or flocculation.

Another growth mechanism, other than particle sintering, has to be proposed. The presence of small particles in the early stages of the reaction is due to rapid nucleation of the original seeds of Ag^0 (step 1). The system is not stabilized until the beginning of particle growth: some larger particles form and a progressive or more sudden shift of mean particle size is observed, depending on the PVP concentration (the reducing ability of the medium). Furthermore, the growth rate of large particles is higher than that of small particles. Small particles then disappear progressively to the benefit of the large ones (step 2). This effect can be related to an Ostwald ripening mechanism, which takes place when the temperature reaches *ca.* 85 °C. The critical particle radius (below which a particle is not stable and dissolves) increases with temperature: as the reaction continues, the smallest particles are no longer stable in solution and dissolve, contributing to the growth of the larger ones.[16] This can be proved by the low reduction rate observed at the beginning of step 3 (Fig. 11): Ag^0 goes on reducing but the simultaneous dissolution of small particles lowers the Ag^0 concentration in solution. The 410 nm peak is then stabilized as long as Ostwald ripening exists. This reaction step is very important, as the system shifts from instability to stability. From this point, the temperature has just reached 120 °C, and the residual silver ions are reduced rapidly.

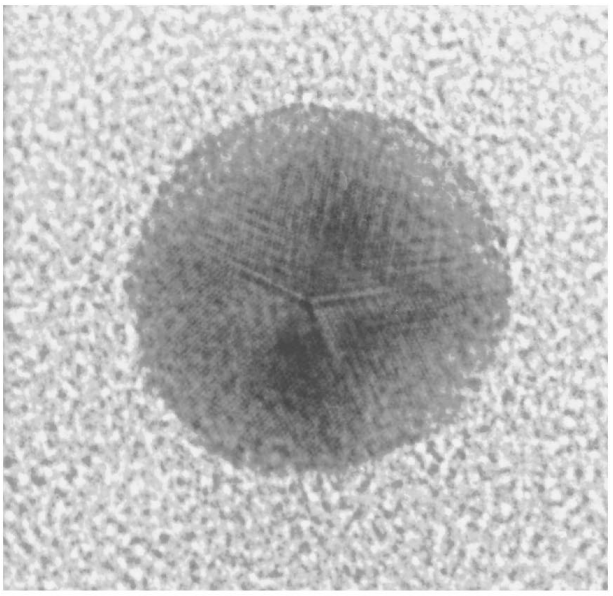

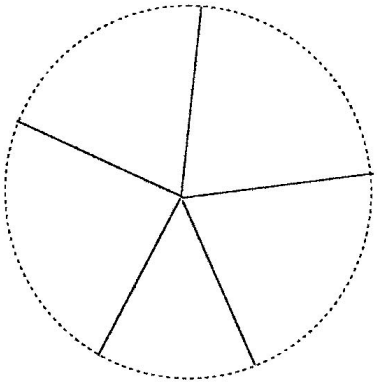

Fig. 13 High-resolution electron micrograph of a colloidal silver particle observed along the [1 1 1] direction and its schematic model

The nucleation and growth processes can be summarized as a schematic representation, based on the general shape of the curve showing the silver ion reduction rate as a function of time. This scheme is proposed in Fig. 14.

Conclusion

Colloidal silver dispersions can be obtained by the polyol process. Strict control of the PVP concentration permits the synthesis of monodisperse colloids. Reaction monitoring and study of the organic phase influence has permitted the characterization of the nucleation and growth process, and enabled a mechanism accounting for the particle formation to be proposed. Particles do not sinter during the reaction, but homogenization and stabilization of the system may be due to Ostwald ripening. However, the variation of temperature during the reaction complicates the interpretation of the kinetic processes and is not ideal for a complete mechanistic understanding. Our work is now dedicated to an isothermal study of our systems, at different reaction temperatures below 120 °C.

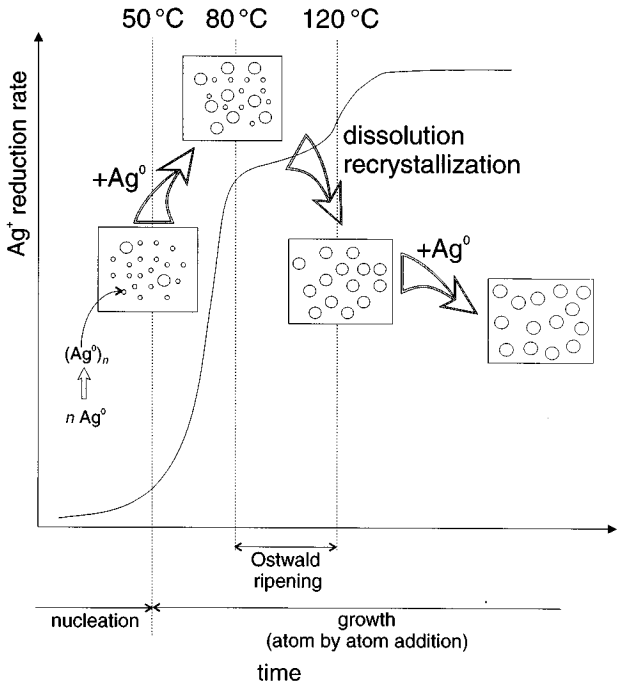

Fig. 14 Scheme showing particle formation

An intriguing question that still remains to be answered is whether such a growth mechanism can be extended to all precious metals. As an attempt to target this issue, the study of various metal–solvent interactions is being pursued.

The authors would like to thank J-M. Tarascon for useful discussions.

References

1 L. N. Lewis and N. Lewis, *Chem. Mater*., 1989, **1**, 106.
2 D. G. Duff, A. C. Curtis, P. P. Edwards, D. A. Jefferson, B. F. G. Johnson and D. E. Logan, *J. Chem. Soc., Chem. Commun*., 1987, **1264**.
3 Z-Y. Huang, G. Mills and B. Hajek, *J. Phys. Chem*., 1993, **97,** 11542.
4 W. P. Halperin, *Rev. Mod. Phys*., 1986, **58**, 533.
5 R. Kubo, A. Kawabata and S. Kobayashi, *Ann. Rev. Mater. Sci*., 1984, **14**, 49.
6 P-Y. Silvert, R. Herrera-Urbina, N. Duvauchelle, V. Vijayakrishnan and K. Tekaia-Elhsissen, *J. Mater. Chem*., 1996, **6**, 573.
7 *Encyclopedia of Polymer Science and Engineering*, 1989, **17**, 204.
8 Z. Zhang, B. Zhao and L. Hu, *J. Solid State Chem*., 1996, **121**, 105–110.
9 K. E. Barret and H. R. Thomas, in *Dispersion Polymerization in Organic Media*, ed. K. E. J. Barret, Wiley, New York, 1975, ch. 4.
10 V. K. La Mer and R. H. Dinegar, *J. Chem. Soc. Jpn*., 1967, **40**, 85.
11 C. Ducamp-Sanguesa, R. Herrera-Urbina and M. Figlarz, *J. Solid State Chem*., 1992, **100**, 272.
12 P. Scherrer, *Nachr. Ges. Wiss. Göttingen*, 1918, 98.
13 L. D. Marks and D. J. Smith, *J. Cryst. Growth*, 1981, **54**, 425.
14 P. L. Gai, M. J. Goringe and J. C. Barry, *J. Microsc*., 1986, **142**, 9.
15 A. I. Kirkland, D. A. Jefferson, D. Tang and P. P. Edwards, *Proc. R. Soc. London A*, 1991, **434**, 279.
16 E. Matijevic, *Chem. Mater*., 1993, **5**, 412.

Paper 6/05347E; *Received* 30*th July*, 1996